Korean J. Chem. Eng., 40(12), 2921-2928 (2023)
DOI: 10.1007/s11814-023-1516-x

pISSN: 0256-1115
eISSN: 1975-7220

Iron-loaded carbon derived from separated microplastics for heterogeneous Fenton degradation of tetracycline hydrochloride

Hongwen Liu*,‡, Xingyang Li*,‡, Guosheng Li*,,†, Yasser Vasseghian***,****,*****,******,†, and Chongqing Wang*,†**

*School of Chemical Engineering, Zhengzhou University, Zhengzhou 450001, China
**Zhongyuan Critical Metals Laboratory, Zhengzhou University, Zhengzhou 450001, China
***Department of Chemistry, Soongsil University, Seoul 06978, South Korea
****School of Engineering, Lebanese American University, Byblos, Lebanon
*****University Centre for Research & Development, Department of Mechanical Engineering, Chandigarh University, Gharuan, Mohali, Punjab, 140413, India
******Department of Sustainable Engineering, Saveetha School of Engineering, SIMATS, Chennai, 602105, India
(*Received 9 May 2023 • Revised 8 June 2023 • Accepted 19 June 2023*)

Abstract−Microplastics are gaining growing research interest due to their significant potential threats to ecosystems and public health. Physical techniques have been proposed as a promising strategy for removing microplastics from the environment. This work innovatively proposes a process of microplastic removal by froth flotation and subsequent carbonization for synthesis of heterogeneous Fenton catalyst. The feasibility of separating different microplastics from water was verified by froth flotation, and iron-loaded carbon derived from separated microplastics was fabricated as catalyst. Carbon material was obtained by carbonization of microplastics, and iron loading was conducted to improve catalytic ability. The catalyst of iron-loaded iron was characterized by scanning electron microscopy and energy-dispersive X-ray spectroscopy. The degradation of tetracycline hydrochloride in the heterogeneous Fenton system was evaluated by single factor experiment and kinetic analysis. The catalytic performance was mainly influenced by H_2O_2 concentration, solution pH, and co-existing ions. Under the conditions of catalyst 20 mg/L, H_2O_2 concentration 0.99 mmol/L, initial tetracycline hydrochloride concentration 20 mg/L, pH 4.0, and temperature 25 °C, the removal rate of tetracycline hydrochloride within 15 min reached 81.6%, and the rate constant was 0.138 min^{-1}. The catalytic mechanism dominated by hydroxyl radical was verified for the degradation of tetracycline hydrochloride. This work offers insights into the management of microplastics and sustainable treatment of antibiotic wastewater.

Keywords: Antibiotic Wastewater, Froth Flotation, Heterogeneous Fenton, Carbonization, Microplastics

INTRODUCTION

Organic wastewater pollution has become a serious environmental problem. These substances can directly or indirectly harm the environment and human health [1,2]. Antibiotics are emerging pollutants that have received widespread attention in recent years. Antibiotics are widely used in industries such as animal feed, pharmaceuticals, and poultry farming [3,4]. The antibiotics in wastewater can cause serious harm to the aquatic ecological environment and human health [5]. Currently, the main methods for the treatment of novel pollutant antibiotics include biodegradation, chemical oxidation, and physical separation. Among them, heterogeneous advanced oxidation processes have been widely studied and applied, and this technology can efficiently decompose antibiotics, transforming them into harmless substances [6,7]. Various materials have been developed and used as heterogeneous catalysts in advanced oxidation processes [8-10]. There is still a high requirement for developing efficient and cheap heterogeneous catalysts.

Microplastics are emerging pollutants in the environment [11,12]. The main sources of microplastics include the use of plastic products and the disposal of plastic wastes [13]. They exist in the natural environment for a long time and continue to accumulate, potentially harming the environment and ecosystem, such as polluting water sources and poisoning the food chain [14]. Various removal technologies have emerged to address the problem of microplastic pollution, such as froth flotation [15], coagulation [16], membrane separation [17], and adsorption [18]. Physical methods have the advantages of simple operation, low cost, and small secondary pollution risk, and have good application prospects for microplastic removal. Jiang et al. [19] used froth flotation to remove microplastics and found that the removal rates of polyvinyl chloride and acrylonitrile butadiene styrene could reach 98.5% when terpineol was 0.219 mg/L and the airflow rate was 7.2 mL/min. Zhang et al. reported that froth flotation was more effective in removing microplastics with high density and large size [20]. Physical techniques have proven to be effective in separating microplastics from the environment, and the disposal of collected microplastics is becoming an essential issue to avoid re-releasing them into the environ-

†To whom correspondence should be addressed.
E-mail: lgscumt@163.com, vasseghian@ssu.ac.kr, zilangwang@126.com
‡Hongwen Liu and Xingyang Li contributed equally to this work.

ment and causing pollution. Plastics have high content of carbon elements in the polymer molecules and can be used as a carbon source to prepare carbon materials. Through processes such as pyrolysis and carbonization of waste plastics, carbon materials with certain structures and properties can be prepared. These carbon materials can be used as materials for organic wastewater treatment and have good application prospects.

This study investigated the removal of microplastics using froth flotation. Carbonization of microplastic and subsequent iron loading were conducted to prepare heterogeneous catalyst for degradation of tetracycline hydrochloride in simulated wastewater. This work provides a strategy of simultaneous treatment of microplastics and antibiotic wastewater.

MATERIALS AND METHODS

1. Materials

Ferric chloride ($FeCl_3$), tetracycline hydrochloride ($C_{22}H_{24}N_2O_8 \cdot HCl$; TCH), tert-butanol ($C_4H_{10}O$; TBA), and o-phenylenediamine ($C_6H_8N_2$) were provided by the Aladdin Bio-Chem Technology (China). Chemicals used in this work were of analytic purity. Microplastic samples of polystyrene (PS), polyethylene terephthalate (PET), and polymethylmethacrylate (PMMA) used for flotation tests were obtained from Dongguan Kemai New Material Co., Ltd, China. PET particles from waste plastics were used to synthesize catalyst.

2. Tests of Froth Flotation

The flotation behavior of microplastics including PS, PMMA, and PET was examined. Suspensions containing microplastics were prepared by mixing a certain amount of microplastics with 100 mL tap water in a 500 mL beaker. The suspension was transferred into the flotation column, and a certain amount of methyl isobutyl carbinol used as frother was added and stirred for 2 min. Then, the air compressor was turned on and the air flow rate (7 mL/min) was adjusted to begin flotation tests. A large number of bubbles were produced by the compressed air passing through the sand core at the bottom of the flotation column. The attachment of microplastic particle and bubbles enabled them float to the top, and the product was collected after sufficient flotation. After drying the product at 60 °C for 10 h, the flotation ratio was calculated according to mass balance [21]. A schematic diagram of flotation process is shown in Fig. 1.

3. Fabrication of Catalyst

PET plastic was mixed with zinc chloride (weight ratio 2 : 1), and the mixture was carbonized in a muffle furnace. The program was set to carbonize for 10 min at 250 °C and 550 °C, respectively, with a heating rate of 10 °C/min. The carbonized product was stirred in HCl solution (0.5 mol/L) for 6 h to remove metals. Then, after rinsing with ultrapure water, filtering, drying at 80 °C for 10 h, and grounding into particles less than 0.15 mm. The obtained carbon material was mixed with Fe^{3+} solution, stirred at 60 °C to remove

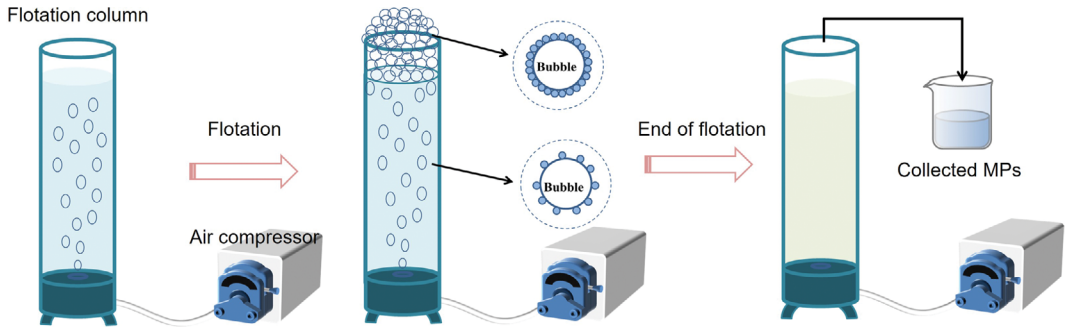

Fig. 1. Schematic diagram of the flotation process.

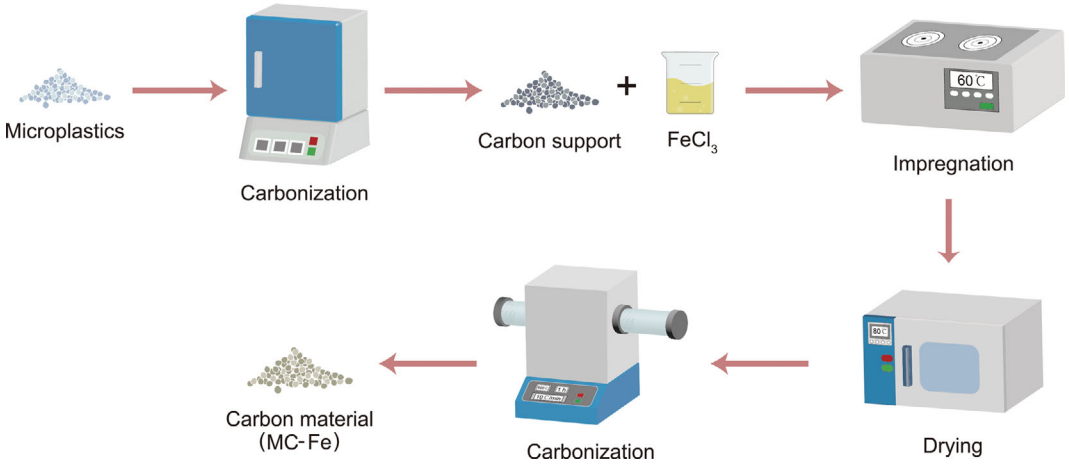

Fig. 2. Flowchart of catalyst preparation.

water, dried at 80 °C for 10 h, and then carbonized at 600 °C for 60 min in a muffle furnace. The iron loaded carbon material (MC-Fe) was obtained and used as catalyst. The preparation process is shown in Fig. 2.

4. Catalytic Tests for TCH Removal

A 50 mL solution of TCH with a concentration of 40 mg/L was placed in a 150 mL conical flask for catalytic experiments. The effects of H_2O_2 amount, pH value, initial TCH concentration, and reaction temperature on the catalytic efficiency were examined under shaking conditions. During the experiments, samples were taken and centrifuged for 1 min using a microcentrifuge. The supernatant was then transferred to a cuvette to record the absorbance at 357 nm using a UV-visible spectrophotometer. The calculation of removal rate, linear fitting of pseudo-first-order kinetic, and calculation of the activation energy are same to our previous study [22].

RESULTS AND DISCUSSION

1. Froth Flotation for Microplastic Removal

The flotation behavior of different microplastics is shown in Fig. 3(a). Preliminary tests proved microplastic particles can be completely removed from water by froth flotation due to large inherent hydrophobicity. The required time for complete removal by froth flotation is 352 s (PS), 108 s (PMMA), 27 s (PET), and 368 s for the mixtures. This suggests that the flotation behavior of microplastics may be related to their physicochemical properties, especially surface wettability [23,24]. Jiang et al. found that the hydrophilicity of different types of microplastics was different during the hydrophilic process of microplastics in the natural environment [25]. The flotation performance of plastic particles is closely related to the bubble formation and abundance, which is predominantly regulated by the addition of a frother. Fig. 3(b) shows the effect of methyl isobutyl carbinol (MIBC) used as frother on PS flotation. The addition of MIBC improves the formation and stability of microbubbles [26], which is helpful for flotation removal of plastic particles. The required time for complete flotation is significantly reduced with addition of more frother. Frother can increase the number of bubbles generated, increase the bubble surface area and carrying capacity, and allow more microplastic particles to adhere to bubble surface [27]. The pictures of the flotation process are shown in Fig. S1. Overall, microplastics in water can be easily removed by froth flotation. However, how to further process the removed microplastics is an emerging challenge. If the collected microplastics are not handled properly, the microplastics may be released back into the environment, causing secondary pollution.

2. Catalyst Synthesis

This work proposes a sustainable strategy for disposal of collected microplastics by physical techniques. Microplastics contain abundant sources of carbon, and research has found that they can be converted into carbon materials through thermochemical processes [28]. This not only solves the problem of microplastic pollution but also converts waste plastics into value-added products. The carbonization of PET in the presence of zinc chloride produces porous carbon, which can be used as support for loading active metal. The reduction of Fe^{3+} occurs during the carbonization of iron loaded carbon, and the iron species with low valence in the catalyst improves the catalytic ability towards hydrogen peroxide for pollutant degradation [22,29]. Fe^{2+} or Fe^0 reacts with H_2O_2 to generate hydroxyl radicals, which has high oxidizability for pollutant degradation. To verify the product of MC-Fe, the morphology and elemental content were analyzed by scanning electron microscopy and energy dispersive spectrometer. The energy dispersive spectrum shows the presence of elements such as carbon, iron, and oxygen in MC-Fe (Fig. S2), indicating that iron has been successfully loaded onto carbon material. From micromorphology, it can be seen the presence of irregular carbon particles, and the small particles on relatively smooth carbon surface may be iron phases (Fig. S3). During carbonization, microplastics are transformed into irregular carbon, and the loaded iron particles provide active sites for hydrogen peroxide activation [28,30].

3. Catalytic Degradation of TCH

TCH is one of the common antibiotics widely existing in aquatic environments. TCH is chosen as target pollutant to examine the catalytic ability of MC-Fe in the presence of H_2O_2. Fig. S4 shows the comparison of TCH removal in different systems. For the addition of only H_2O_2, TCH concentration is nearly unchanged for reaction 15 min, and this can be ascribed to the poor oxidizing ability of H_2O_2. In the presence of only MC-Fe, the concentration of TCH is minorly declined after reaction 15 min, implying the

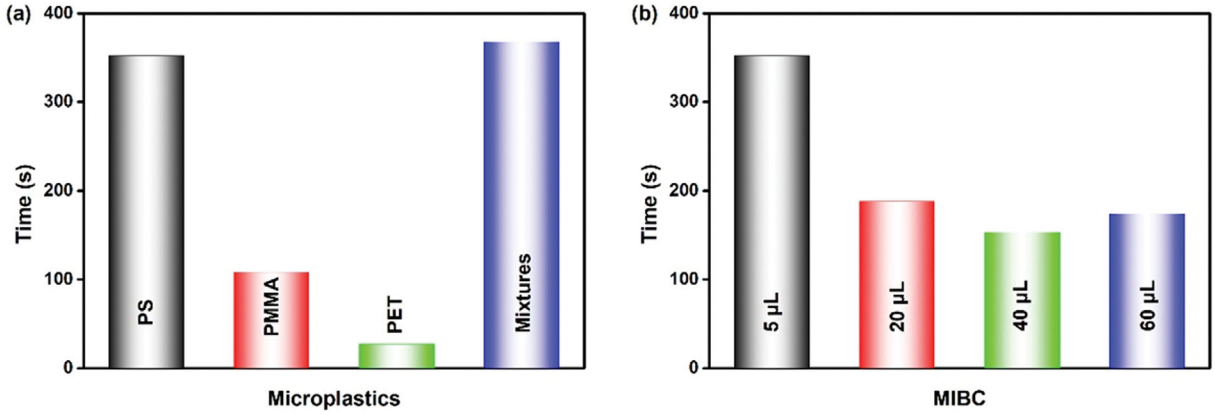

Fig. 3. (a) The required time for complete removal of different microplastics by froth flotation, (b) the effect of frother addition on PS flotation.

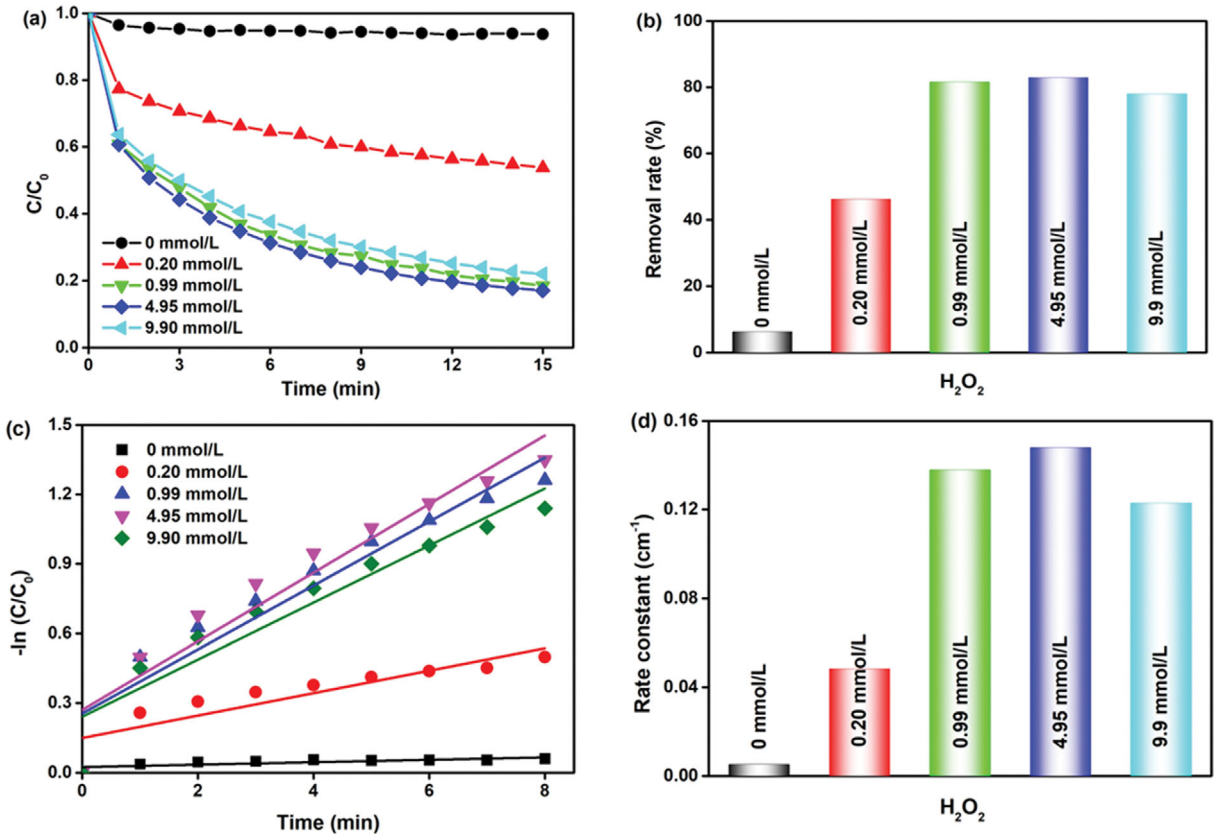

Fig. 4. (a) Effect of H_2O_2 concentration on TCH degradation, (b) the removal rate of TCH at 15 min, (c) linear fitting of kinetic model, and (d) the value of rate constants (MC-Fe 20 mg/L, pH 4.0, initial TCH concentration 40 mg/L, temperature 25 °C).

poor adsorption impact of MC-Fe for TCH removal. This can be ascribed to low surface area and fewer adsorption sites on MC-Fe surface [31]. TCH concentration rapidly decreased in MC-Fe/H_2O_2 system, and 81.6% of TCH was removed within 15 min. This suggests the high catalytic ability of MC-Fe. The heterogeneous Fenton degradation of TCH using different catalysts is compared in Table S1, and it can be observed that MC-Fe is superior or comparable to other well-designed catalysts.

3-1. Effect of H_2O_2 Concentration

Fig. 4 shows the impact of H_2O_2 concentration on TCH degradation. TCH concentration decreases with reaction time, and the addition of H_2O_2 improves TCH removal. Increasing H_2O_2 from 0 to 0.99 mmol/L significantly enhances the degradation of TCH molecules, while further adding more H_2O_2 does improve TCH degradation and even lowers the degradation process. The removal rates of TCH at 15 min are 6.3% (0 mmol/L), 46.2% (0.20 mmol/L), 81.6% (0.99 mmol/L), 82.9% (4.95 mmol/L), and 78.0% (9.90 mmol/L). The relationship between $-\ln(C_t/C_0)$ and reaction time t is linear, implying that TCH degradation can be well fitted by the pseudo-first-order kinetic. This agrees well with previous reports [32]. When the H_2O_2 concentration is 0 mmol/L, 0.20 mmol/L, 0.99 mmol/L, 4.95 mmol/L, and 9.90 mmol/L, the rate constants are 0.005 min^{-1}, 0.048 min^{-1}, 0.138 min^{-1}, 0.148 min^{-1}, and 0.123 min^{-1}, respectively. At low concentration of H_2O_2, the addition of H_2O_2 makes a significant contribution to TCH degradation due to the generation of more $^{\bullet}OH$ through H_2O_2 activation by MC-Fe catalyst. After saturation concentration, the increase of H_2O_2 does not improve TCH degradation. Additionally, the excessive H_2O_2 has an inhibitory effect on $^{\bullet}OH$ generation, and excess $^{\bullet}OH$ may be consumed by side reactions [33,34]. The H_2O_2 concentration of 0.99 mmol/L was chosen for subsequent experiments.

3-2. Effect of Initial pH Value

The impact of initial pH on TCH removal is demonstrated in Fig. 5. TCH concentration decreases with reaction time at pH 4.0. When the initial pH is increased from 4.0 to 11.0, TCH removal is significantly lowered. The removal rates of TCH within at pH of 4.0, 7.0, 9.0, and 11.0 are 81.6%, 54.6%, 39.0%, and 19.2%, respectively. The rate constants are 0.138 min^{-1}, 0.062 min^{-1}, 0.036 min^{-1}, and 0.016 min^{-1} at pH 4.0, 7.0, 9.0, and 11.0. Fenton reactions occur at optimal pH around 3.5. Acidic condition favors iron leaching and Fenton reactions, thus generating more $^{\bullet}OH$ for TCH degradation. Moreover, H^+ in acidic solution reacts with H_2O_2 to generate $H_3O_2^+$, which enhances the stability of H_2O_2 and suppresses the production of $^{\bullet}OH$ [35]. When the solution pH is higher than 4.0, the removal rate of TCH decreases, which is due to the precipitation of Fe^{3+} at solution pH higher than 4.0 and Fe^{2+} at solution pH higher than 6.0, which adheres to the surface of the catalyst, affecting the contact between active sites and pollutants, and reducing the catalytic ability [36]. The formation equation of iron hydroxide is shown as Eqs. (1)-(5) [37]. In previous studies, high catalytic ability at low pH was reported for Sun et al. [30]. MC-Fe exhibits good catalytic ability at 4.0, and further research should be con-

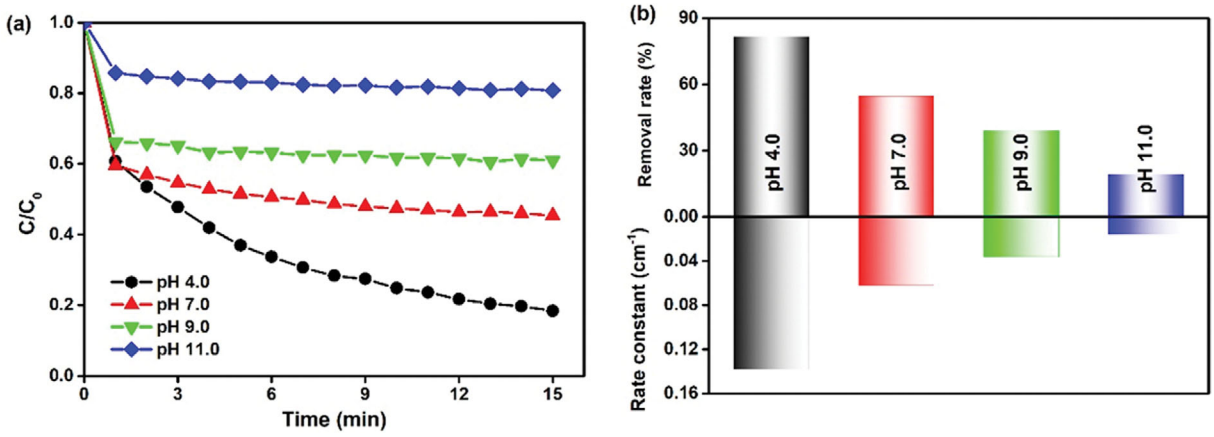

Fig. 5. (a) Effect of initial pH on TCH degradation, (b) the removal rate of TCH at 15 min, (c) linear fitting of kinetic model, and (d) the value of rate constants (H_2O_2 0.99 mmol/L, MC-Fe 20 mg/L, initial TCH concentration 40 mg/L, temperature 25 °C).

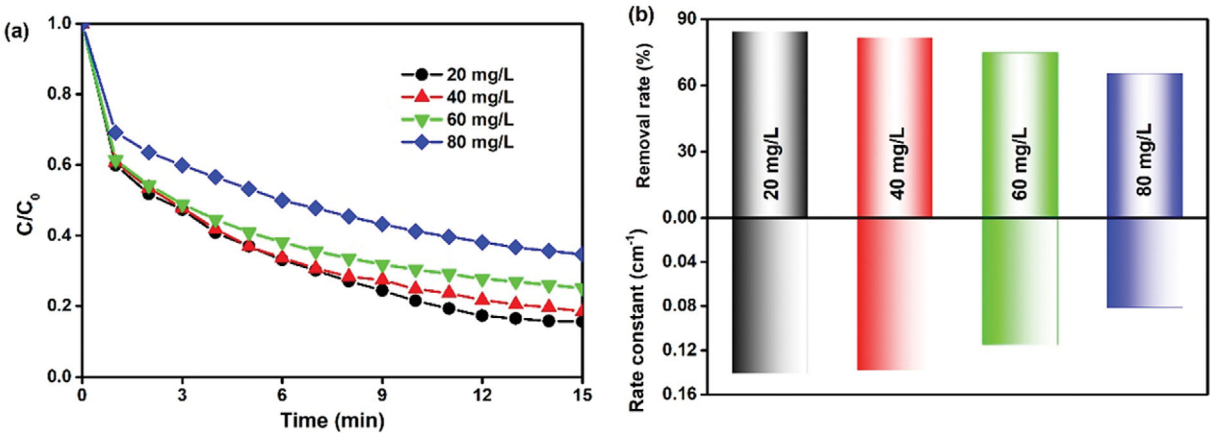

Fig. 6. (a) Effect of initial TCH concentration on TCH degradation, (b) the removal rate of TCH at 15 min, (c) linear fitting of kinetic model, and (d) the value of rate constants (H_2O_2 0.99 mmol/L, MC-Fe 20 mg/L, pH 4.0, temperature 25 °C).

ducted to broaden operation pH for TCH degradation.

$$Fe^{2+}+H_2O_2 \rightarrow Fe^{3+}+{}^{\bullet}OH+OH^- \quad (1)$$

$$Fe^{2+}+H_2O \rightarrow FeOH^{+}+2H^{+} \ (k=1.9\ s^{-1}) \quad (2)$$

$$Fe^{3+}+H_2O \rightarrow FeOH^{2+}+H^{+} \ (k=2.3\times10^{-7}\ s^{-1}) \quad (3)$$

$$Fe^{3+}+2\ H_2O \rightarrow Fe(OH)_2^{+}+2H^{+} \ (k=4.7\times10^{-7}\ s^{-1}) \quad (4)$$

$$2Fe^{3+}+2\ H_2O \rightarrow Fe_2(OH)_2^{4+}+2H^{+} \ (k=1.1\times10^{-7}\ s^{-1}) \quad (5)$$

3-3. Effect of Initial TCH Concentration

Fig. 6 shows TCH degradation under different initial concentrations. It can be seen that the increasing initial concentration results in lower TCH removal. The removal rates at 15 min of TCH at initial concentrations of 20 mg/L, 40 mg/L, 60 mg/L, and 80 mg/L are 84.4%, 81.6%, 74.8%, and 65.4%, respectively. The linear fitting of kinetic model gives the rate constants. The rate constants are 0.1406 min^{-1}, 0.1379 min^{-1}, 0.1148 min^{-1}, and 0.0812 min^{-1}, respectively. The negative impact of high TCH concentration can be explained from two aspects. When the addition of MC-Fe catalyst and H_2O_2 is designed, the amount of active species generated by catalytic reactions is constant, and thus there is an upper limit to the removal of TCH. In addition, at high TCH concentration, excessive TCH molecules or degradation intermediates may adsorb on the surface of MC-Fe, occupying the active sites of the catalyst, hindering the reactions between MC-Fe and H_2O_2, and causing a decrease in TCH degradation. As to wastewater with high TCH concentration, an effective process can be realized by increasing reaction time.

3-4. Effect of Reaction Temperature

From Fig. 7, the impact of temperature on TCH degradation can be seen. Increasing temperature slightly improves TCH degradation. The removal rates of TCH at 10 min are 75.2% (25 °C), 79.1% (35 °C), 82.3% (45 °C), and 83.2% (55 °C). A slight increase of rate constant is also observed when the temperature increases from 25 °C to 55 °C. The positive effect of temperature on TCH degradation may be since increasing temperature can accelerate the molecular motion in the solution, thereby accelerating the reaction rate of TCH degradation. Previous studies reported similar results of improving pollutant degradation at higher temperatures. In MC-Fe/H_2O_2 system, the contribution of reaction temperature to TCH degradation is minor. And TCH degradation can be achieved at room temperature without energy consumption at higher temperature.

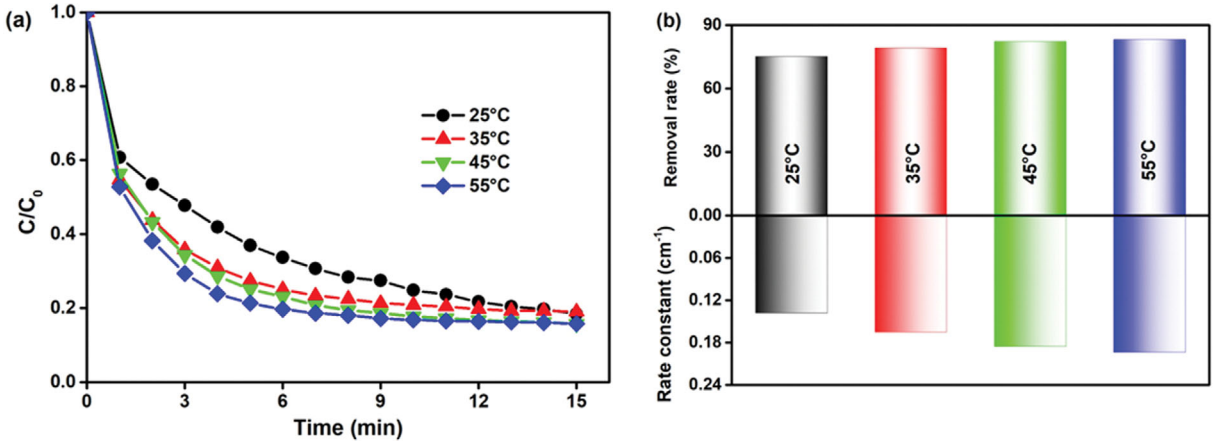

Fig. 7. (a) Effect of reaction temperature on TCH degradation, (b) the removal rate of TCH at 10 min, (c) linear fitting of kinetic model, and (d) the value of rate constants (H_2O_2 0.99 mmol/L, MC-Fe 20 mg/L, pH 4.0, initial TCH concentration 40 mg/L).

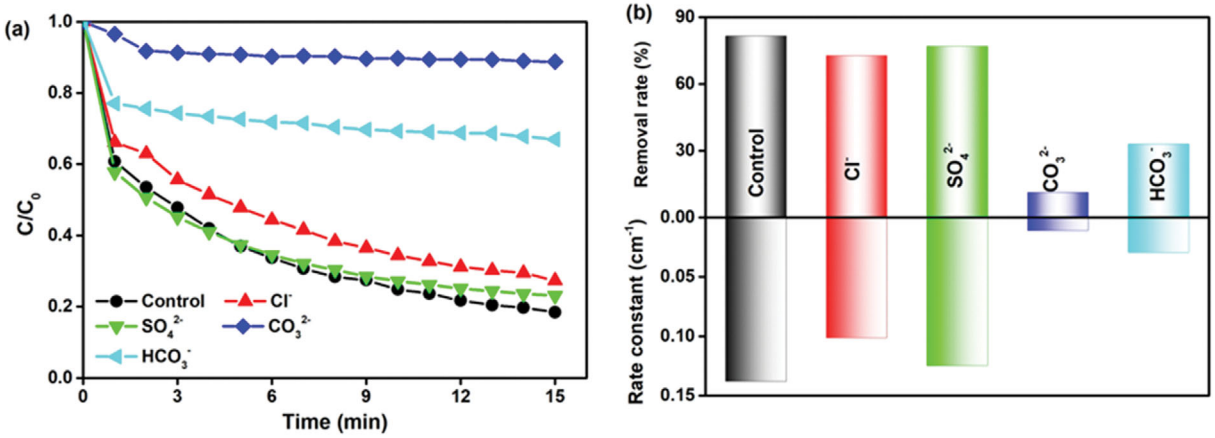

Fig. 8. (a) Effect of anions on TCH degradation, (b) the removal rate of TCH at 15 min and the value of rate constants (H_2O_2 0.99 mmol/L, MC-Fe 20 mg/L, pH 4.0, initial TCH concentration 40 mg/L, temperature 25 °C).

3-5. Effect of Co-existing Anions

There are co-existing ions in a real aquatic environment. It has been reported that anions may influence the pollutant degradation in the heterogeneous Fenton process [38]. To examine the impact of co-existing anions, TCH degradation in the presence of common anions including CO_3^{2-}, HCO_3^-, Cl^-, and SO_4^{2-} was conducted (Fig. 8). The anions exhibit different impacts on the removal of TCH. Compared to Cl^- and SO_4^{2-}, CO_3^{2-} and HCO_3^- manifest significant inhibition on TCH removal. The removal rates of TCH at 15 min are 81.6% (no anion), 72.7% (Cl^-), 77.0% (SO_4^{2-}), 11.3% (CO_3^{2-}), and 33.0% (HCO_3^-), respectively. As to the rate constant, it follows the order: SO_4^{2-}>Cl^->HCO_3^->CO_3^{2-}. The inhibitory effect of CO_3^{2-} and HCO_3^- can be ascribed to the consumption of the generated hydroxyl radical (Eqs. (6)-(7)) and elevated solution pH [39]. In Huang's study, Cl^- could compete to consume $^{\bullet}OH$, but the inhibition effect of Cl^- on tetracycline degradation was very weak, only decreasing from 91.34% to 85.69% [40]. Studies have shown that the effect of inorganic anions on pollutant degradation may depend on their initial concentration [29]. It was found that chloride ions had an obvious inhibitory effect only at high concentration (Eqs. (8)-(10)) in the process of removing sulfamethoxazole, while for bicarbonate and carbonate ions, high concentration would enhance the pollutant removal [41].

$$HCO_3^- + {}^{\bullet}OH \rightarrow CO_3^{\bullet-} + H_2O \quad (6)$$

$$CO_3^{2-} + {}^{\bullet}OH \rightarrow CO_3^{\bullet-} + OH^- \quad (7)$$

$$Cl^- + {}^{\bullet}OH \rightarrow ClOH^{\bullet-} \quad (8)$$

$$ClOH^{\bullet-} + H^+ \rightarrow Cl^{\bullet} + H_2O \quad (9)$$

$$ClOH^{\bullet-} + Cl^- \rightarrow Cl_2^{\bullet-} + OH^- \quad (10)$$

4. Catalytic Mechanism

Quenching tests using radical scavenger have been identified as effective for identifying the role of radicals in pollutant degradation in heterogeneous Fenton process [42,43]. TBA is an efficient scavenger of $^{\bullet}OH$, and its reaction rate constant with $^{\bullet}OH$ is as high as 6×10^8 mol^{-1} s^{-1} [44]. To verify whether TCH removal in the system is caused by $^{\bullet}OH$, the effect of TBA addition on TCH degradation was studied and shown in Fig. 9(a). In the presence of TBA, TCH degradation is remarkably inhibited, and the removal

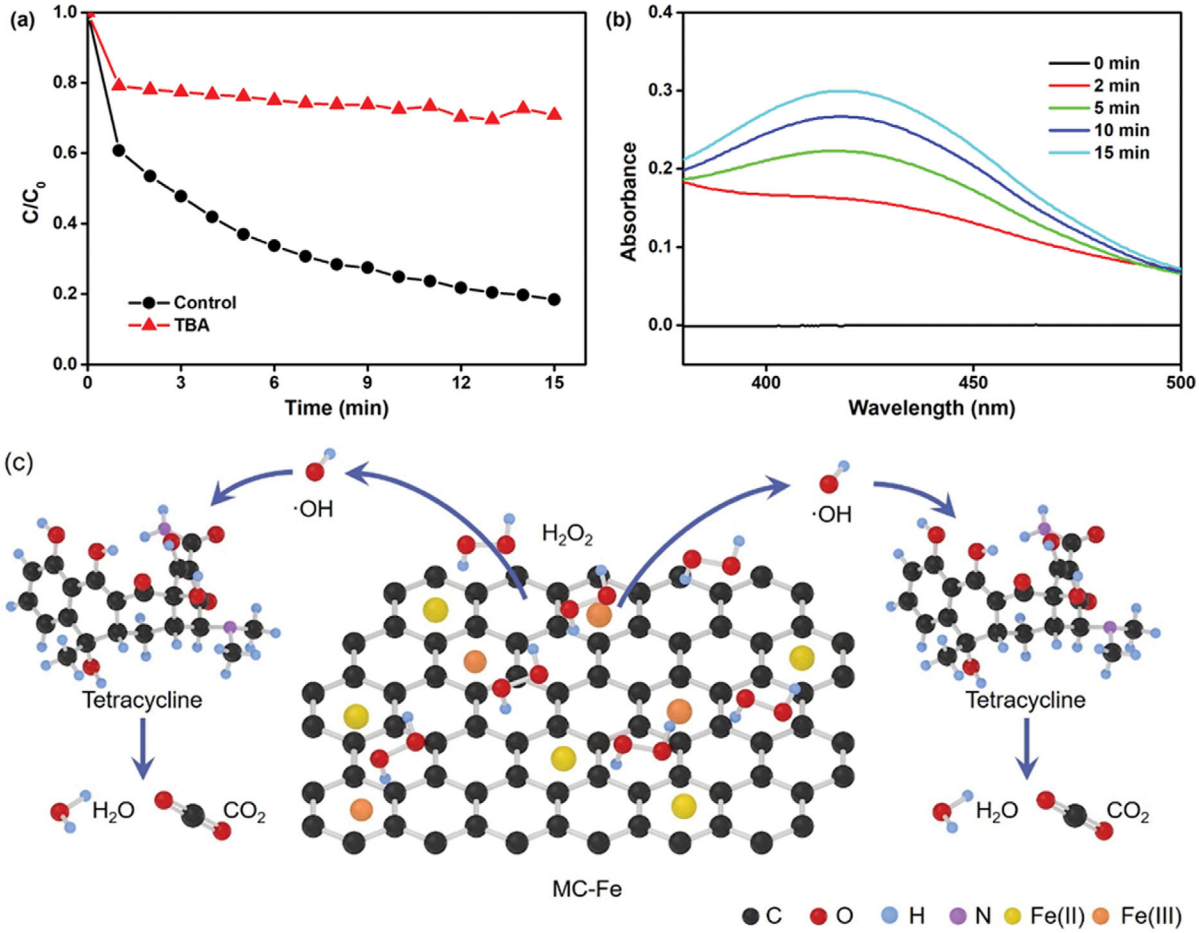

Fig. 9. (a) Effect of TBA addition on TCH degradation, (b) the UV spectrum in the presence of ortho-phenylenediamine, (c) the tentative mechanism of TCH degradation in MC-Fe/H_2O_2 system.

rate at 15 min is decreased from 81.6% to 29.2%. The proves the important role of $^{\bullet}OH$ for TCH degradation in the MC-Fe/H_2O_2 system [29]. After adding TBA, TCH degradation is not fully inhibited, and this can be the existence of other reactive species such as $^{\bullet}OOH$ and $O_2^{\bullet-}$ [45]. The presence of $^{\bullet}OH$ in the MC-Fe/H_2O_2 system is further verified by UV spectrophotometry [46]. Ortho-phenylenediamine reacts with $^{\bullet}OH$, and the product can be identified by the UV spectrum. The absorbance at 420 nm shown in Fig. 9(b) verifies the existence of $^{\bullet}OH$. The intensity of absorbance increases with prolonging reaction time, indicating the formation of more $^{\bullet}OH$. According to the above results, a tentative mechanism of TCH degradation in MC-Fe/H_2O_2 system can be illustrated in Fig. 9(c). The loaded iron in MC-Fe partially leaches under acidic condition, and the iron ions react with H_2O_2 to generate $^{\bullet}OH$, which results in the decomposition and mineralization of TCH molecules into inorganic species such as CO_2 and H_2O [47]. Also, the iron on catalyst surface can react with H_2O_2 to produce $^{\bullet}OH$ for TCH degradation.

CONCLUSIONS

This work provides an effective strategy for management of microplastics. Froth flotation is effective for removing different microplastics from water. The microplastics can be converted iron loaded carbon as heterogeneous Fenton catalyst for catalytic degradation of antibiotics. TCH degradation in the catalytic system is influenced by process factors including H_2O_2 concentration, solution pH, initial TCH concentration, reaction temperature, and co-existing ions. Under the conditions of MC-Fe 20 mg/L, H_2O_2 concentration 0.99 mmol/L, initial TCH concentration 20 mg/L, pH 4.0, and temperature 25 °C, the removal rate of TCH within 15 min reached 81.6%, and the rate constant was 0.138 min^{-1}. The catalytic mechanism dominated by hydroxyl radical was verified for the degradation of TCH. The proposed process simultaneously solves the problem of emerging pollutants, including microplastics and antibiotics. Future researches should be conducted to optimize catalyst synthesis and apply it to real wastewater treatment.

DECLARATION OF INTEREST

The authors declare that they have no known competing financial interests or personal relationships that could have appeared to influence the work reported in this paper.

SUPPORTING INFORMATION

Additional information as noted in the text. This information is

available via the Internet at http://www.springer.com/chemistry/journal/11814.

REFERENCES

1. L. Wang, D. Luo, O. Hamdaoui, Y. Vasseghian, M. Momotko, G. Boczkaj and C. Wang, *Sci. Total Environ.*, **876**, 162551 (2023).
2. C. G. Joseph, Y. H. Taufiq-Yap, N. A. Affandi, J. L. H. Nga and V. Vijayan, *Korean J. Chem. Eng.*, **39**(3), 484 (2022).
3. K. Tian, L. Hu, L. Li, Q. Zheng, Y. Xin and G. Zhang, *Chin. Chem. Lett.*, **33**(10), 4461 (2022).
4. M. A. Uddin, B. H. Sutonu, M. A. Rub, S. Mahbub, M. M. Alotaibi, A. M. Asiri and M. Kabir, *Korean J. Chem. Eng.*, **39**(3), 664 (2022).
5. A. Balakrishnan, M. Chinthala, R. K. Polagani and D.-V. N. Vo, *Environ. Res.*, **216**(Pt 3), 114660 (2023).
6. A. R. Bracamontes-Ruelas, L. A. Ordaz-Díaz, A. M. Bailón-Salas, J. C. Ríos-Saucedo, Y. Reyes-Vidal and L. Reynoso-Cuevas, *Processes*, **10**(5), 1041 (2022).
7. L. Wang, H. Jiang, H. Wang, P. L. Show, A. Ivanets, D. Luo and C. Wang, *J. Environ. Chem. Eng.*, **10**(6), 108954 (2022).
8. A. Hojjati-Najafabadi, A. Aygun, R. N. E. Tiri, F. Gulbagca, M. I. Lounissaa, P. Feng and F. Sen, *Ind. Eng. Chem. Res.*, **62**(11), 4655 (2023).
9. E. Baladi, F. Davar and A. Hojjati-Najafabadi, *Environ. Res.*, **215**, 114270 (2022).
10. M. Mansoorianfar, H. Nabipour, F. Pahlevani, Y. Zhao, Z. Hussain, A. Hojjati-Najafabadi and R. Pei, *Environ. Res.*, **214**(Pt 4), 114113 (2022).
11. M. A. Browne, P. Crump, S. J. Niven, E. Teuten, A. Tonkin, T. Galloway and R. Thompson, *Environ. Sci. Technol.*, **45**(21), 9175 (2011).
12. Y. J. Lee, J. W. Yang, B. Choi, S. J. Park, C. G. Lee and E. H. Jho, *Korean J. Chem. Eng.*, **40**(3), 612 (2023).
13. C. M. Rochman, *Science*, **360**(6384), 28 (2018).
14. H. Golwala, X. Zhang, S. M. Iskander and A. L. Smith, *Sci. Total Environ.*, **769**, 144581 (2021).
15. Y. Zhang, H. Jiang, K. Bian, H. Wang and C. Wang, *Sci. Total Environ.*, **792**, 148345 (2021).
16. G. Zhou, Q. Wang, J. Li, Q. Li, H. Xu, Q. Ye, Y. Wang, S. Shu and J. Zhang, *Sci. Total Environ.*, **752**, 141837 (2021).
17. M. Malankowska, C. Echaide-Gorriz and J. Coronas, *Environ. Sci.: Water Res. Technol.*, **7**(2), 243 (2021).
18. L. Fu, J. Li, G. Wang, Y. Luan and W. Dai, *Ecotoxicol. Environ. Saf.*, **217**, 112207 (2021).
19. H. Jiang, Y. Zhang, K. Bian, H. Wang and C. Wang, *J. Environ. Chem. Eng.*, **10**(3), 107834 (2022).
20. Y. Zhang, H. Jiang, K. Bian, H. Wang and C. Wang, *J. Environ. Chem. Eng.*, **9**(4), 105463 (2021).
21. H. Jiang, Y. Zhang, K. Bian, C. Wang, X. Xie, H. Wang and H. Zhao, *Chem. Eng. J.*, **448**, 137692 (2022).
22. C. Wang, R. Sun and R. Huang, *J. Cleaner Prod.*, **297**, 126681 (2021).
23. H. Wang, C. Wang, J. Fu and G. Gu, *Colloids Surf., A.*, **424**, 10 (2013).
24. H. Feilin and S. Mingwei, *Process Saf. Environ. Prot.*, **168**, 613 (2022).
25. H. Jiang, J. Bu, K. Bian, J. Su, Z. Wang, H. Sun, H. Wang, Y. Zhang and C. Wang, *Water Res.*, **233**, 119794 (2023).
26. Y. Pan, I. Gresham, G. Bournival, S. Prescott and S. Ata, *Powder Technol.*, **397**, 117028 (2022).
27. A. Bahrami, Y. Ghorbani, M. R. Hosseini, F. Kazemi, M. Abdollahi and A. Danesh, *Mining Metall. Explor.*, **36**(2), 409 (2019).
28. C. Wang, R. Huang, R. Sun, J. Yang and D. D. Dionysiou, *J. Cleaner Prod.*, **330**, 129901 (2022).
29. C. Wang, R. Sun, R. Huang and H. Wang, *Sep. Purif. Technol.*, **270**, 118773 (2021).
30. R. Sun, X. Zhang, C. Wang and Y. Cao, *J. Environ. Chem. Eng.*, **9**(4), 105368 (2021).
31. J. Dai, X. Meng, Y. Zhang and Y. Huang, *Bioresour. Technol.*, **311**, 123455 (2020).
32. C. Wang, J. Yang, R. Huang and Y. Cao, *J. Cent. South Univ.*, **29**(12), 3884 (2022).
33. M. Cheng, Y. Liu, D. Huang, C. Lai, G. Zeng, J. Huang, Z. Liu, C. Zhang, C. Zhou, L. Qi, W. Xiong, H. Yi and Y. Yang, *Chem. Eng. J.*, **362**, 865 (2019).
34. Y. Ren, J. Yu, J. Zhang, L. Lv and W. Zhang, *Appl. Catal., B.*, **299**, 120697 (2021).
35. X. Sun, X. Ni, X. Wang and D. Xu, *Surf. Interfaces*, **31**, 102053 (2022).
36. M. González-Davila, J. M. Santana-Casiano and F. J. Millero, *Geochim. Cosmochim. Acta*, **69**(1), 83 (2005).
37. S. Chen, P. Xiong, W. Zhan and L. Xiong, *Miner. Eng.*, **122**, 38 (2018).
38. L. Wang, D. Luo, J. Yang and C. Wang, *J. Cleaner Prod.*, **375**, 134118 (2022).
39. L. Hu, G. Zhang, M. Liu, Q. Wang and P. Wang, *Chem. Eng. J.*, **338**, 300 (2018).
40. J. Huang, M. Wang, S. Luo, Z. Li and Y. Ge, *Environ. Res.*, **219**, 115166 (2023).
41. S. Wang and J. Wang, *Chem. Eng. J.*, **351**, 688 (2018).
42. D.-H. Xie, P.-C. Guo, K.-Q. Zhong and G.-P. Sheng, *Appl. Catal., B.*, **319**, 121923 (2022).
43. H.-Y. Xu, Y. Xu, S.-Q. Zhang, L.-Y. Dai and Y. Wang, *Mater. Lett.*, **337**, 133985 (2023).
44. Y. Zhu, Q. Xie, R. Zhu, Y. Lv, Y. Xi, J. Zhu and J. Fan, *Chemosphere*, **287**, 131933 (2022).
45. Y. Liu, J. Li, L. Wu, D. Wan, Y. Shi, Q. He and J. Chen, *Sci. Total Environ.*, **761**, 143956 (2021).
46. X. Li, X. Zhang, S. Wang, P. Yu, Y. Xu and Y. Sun, *J. Environ. Manage.*, **312**, 114856 (2022).
47. W. Hua and Y. Kang, *Korean J. Chem. Eng.*, **40**(5), 1122 (2023).